



Research on mining-induced deformation and stress, insights from physical modeling and theoretical analysis

Guodong Li¹ · Shugang Cao² · Feng Luo¹ · Yong Li² · Yaxing Wei¹

Received: 18 October 2017 / Accepted: 30 January 2018 / Published online: 6 March 2018
© Saudi Society for Geosciences 2018

Abstract

The dynamic change of mining-induced stress is the main reason for large deformation of surrounding rock. To investigate the influence of mining-induced stress and deformation is important for appropriate supportive design. It also helps to raise the safety and productivity of longwall mining operations. In this paper, Weijiagou Coal Mine in Southwest China was selected as the case study. In order to research on the deformation and breakage of overlying strata, physical modeling test was carried out on the self-developed rotatable physical similar test system. By using digital image correlation (DIC) technique, the deformation of strata and development of cracks in the process of coal seam excavation were acquired, meanwhile, mining-induced stress was also monitored by pressure cell and strainmeter. According to the mechanical structure of stope, the height of the destressed zone has a significant influence on stress distribution. In order to minimize the discrepancy between the physical model test and theoretical analysis, the dimension of the plastic zone of roadway was added into the mining panel width, and the gap between the experimental and theoretical results reduced.

Keywords Mining-induced stress · Stress concentration · Strata deformation · Physical modeling

Introduction

Coal seam mining causes redistribution of underground stress which is uniformly distributed in surrounding rock before coal seam excavation. Some area in stope become destressed (e.g., the strata above goaf), while the adjacent neighboring solid sections become stress-concentrated (e.g., the coal seam ahead of working face). Accordingly, it could be considered that there is in situ and mining-induced stress in surrounding rock after coal seam excavation (Singh and Singh 2010). Moreover, with working face advancing, the mining-induced stress dynamically changes both in space and in time. The distribution of mining-induced stress, especially the location

and amount of maximum, is important for supportive design and safety production. But, it is not easy to make a clear understanding of it. The geological condition of strata, the value of in situ stress, and the mechanical properties of surrounding rock all have a significant influence on distribution mining-induced stress. Besides, the adopted mining technique, the dimension of mining panel, the advancing speed of working face, etc. are other important factors (Feng 2015).

Generally, theoretical analysis, in situ test, physical modeling, and numerical simulation are utilized by researchers to study the development of mining-induced stress (Salamon 1984; Ju et al. 2017; Wang et al. 2016; Toraño et al. 2002). But, in situ test is more time-consuming and expensive. The empirical rules base on past experiences do provide a general guide; however, the heterogeneous nature of mine geology may result in errors. On the contrast, the physical experiment and theoretical analysis are more adoptable.

In this research, theoretical analysis was carried out to study the height of the destressed zone and stress concentration factor in the context of Weijiagou Coal Mine in Southwest China. Meanwhile, physical modeling experiment was also used to study the deformation of strata and the development of mining-induced crack and stress.

✉ Shugang Cao
shugang.cao@cqu.edu.cn

¹ School of Mining and Geomatics, Hebei University of Engineering, Handan, Hebei 056038, China

² State Key Laboratory of Coal Mine Disaster Dynamics and Control, Chongqing University, Chongqing 400044, China

Stress distribution around longwall mining panel

Many scholars carried out experiments and analysis to study mining-induced stress in the situation of longwall mining. By supposing the coal seam was infinite, elastic, isotropic, and homogenous, Salamon (1984) developed an analytical equation to evaluate the stress distribution at the edge of longwall panel. Ju et al. (2017) and Wang et al. (2016) studied the characteristics of overlying strata collapse and mining-induced pressure by employing the physical model test. By numerical modeling, Toraño (2002) proved that the concentration factor of mining-induced stress around roadway is approximately 2.3 times of in situ stress. Yavuz (2004) demonstrated that mining height had a positive correlation with the distance of working face to abutment stress. Based on stress evolution both in time and space during longwall mining, Yang et al. (2011) found that the abutment stress changed rapidly within 10 m in front of working face, and the maximum value was approximately twice the in situ stress when the mining size reached 20–30 m. The finite element modeling performed by Khanal et al. (2011); Khanal and Adhikary (2012) demonstrated that the maximum induced vertical stress is approximately four times of the in situ stress. According to the above researches, it can be found that many methods are available to study the mining-induced stress. However, the results obtained from these methods are discrete. A major task is to select a more reliable and intended way to perform a realistic assessment. Additionally, the geological condition of a coal mine is non-uniform and complex, which makes it a challenge to study the distribution and variation of mining-induced stress.

Time-dependent energy model

The transfer of mining-induced stress in strata

The coal seam excavation causes stress redistribution and results in degeneration of integrity of surrounding rock. Generally, according to the deformation and damage state, the overburden strata of goaf could be classified into three regions: caved region, fractured region, and bending region from bottom to top. Because stress in the former two regions has almost totally stress released, this area can be named “destressed zone,” as shown in Fig. 1. The weight of strata above the destressed zone transfers to adjacent coal seam and rock mass. Meanwhile, the abutment strata on the lateral of the destressed zone are the media for stress transfer. As the height of the destressed zone (H_d) increases, the volume of overlying strata and the mining-induced stress reduces. So, H_d is the main influence factor to calculate mining-induced stress.

Energy conservation in stope

The combination of coal seam and surrounding rock can be seemed as an enclosing system. Coal seam excavation undermines the balance within the system. The strain energy stored in excavated coal seam shifts, enriches, and rebalances again in other area. Actually, the concentration of stress in coal and rock mass can also be considered as energy accumulation. Based on the law of energy conservation, the total strain energy stored in the mined material is released and consumed in overlying and underlying strata deforming, fracturing, and caving. Therefore, the stored strain energy in the mined material (U_m) should be equal to the stored strain energy of caved material within the destressed zone (U_d) (Rezaei et al. 2015a).

$$U_d = U_m \tag{1}$$

U_m can be calculated by the following equation:

$$U_m = \frac{(1 + \nu)(1-2\nu)}{2(1-\nu)E} \gamma A_m \sigma_v \left(\frac{h_s^2}{3} + H^2 + Hh_s \right) \tag{2}$$

where ν is Poisson’s ratio of rock mass, E is the elastic modulus of excavated material, γ is the volume weight of rock mass, A_m is the cross-section area of the mined panel, σ_v is the vertical-induced stress, h_s is the mining height, and H is the depth of cover.

In general, U_d is composed of elastic strain energy and viscoplastic strain energy:

$$U_d = \frac{A_d H_d \sigma_c^2}{2 \left(E + \frac{b_1 \sigma_c}{b_1 - 1} \right)} \left(2Ee^{-bt} + \frac{\sigma_s^\mu}{Bt^\omega} - \lambda \right) \tag{3}$$

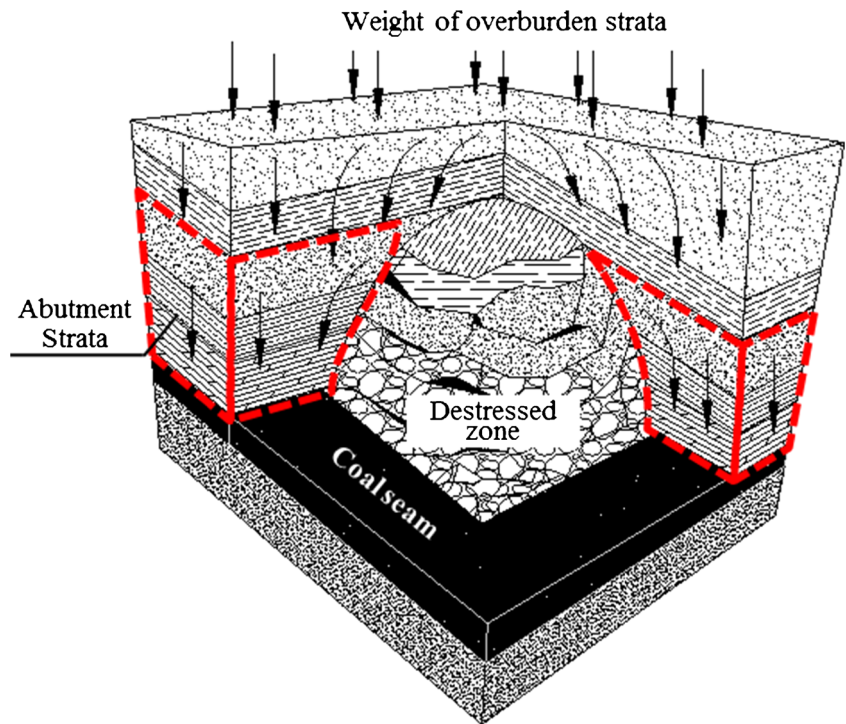
Where A_d is the unit surface of goaf area, σ_c is uniaxial compressive strength of caved material, b_1 is the bulking factor, σ_s is the threshold value of stress, B is the material constant related to viscosity and temperature, t is the pressure time of caved material, λ is the slope of material hardening stage, and $b, \omega,$ and μ are material constants.

Accordingly, the substitution of eq. (2) and (3) into (1) yield the equation for calculating H_d in long-term or time-dependent condition (Rezaei et al. 2015b).

$$H_d = \frac{\gamma A_m \sigma_v (1 + \nu)(1-2\nu) \left(E + \frac{b_1 \sigma_c}{b_1 - 1} \right)^2 \left(\frac{h_s^2}{3} + H^2 + Hh_s \right)}{A_d E \sigma_c^2 (1-\nu) \left(2Ee^{-bt} + \frac{\sigma_s^\mu}{Bt^\omega} - \lambda \right)} \tag{4}$$

where σ_v is the vertical mining-induced stress and b_1 is the bulking factor of rock.

Fig. 1 Schematic of stress transfer in longwall mining



Beyond the height of the destressed zone, the ground stress transfers to the front abutment strata and adjacent coal seam. In vertical direction, the mining-induced stress applied by

abutment rock mass σ_{av} can be obtained by the following equation (Hou and Ma 1989).

$$\sigma_{av} = \left(\frac{\gamma A_m \sigma_v (1 + \nu) (1 - 2\nu) \left(E + \frac{b_1 \sigma_c}{b_1 - 1} \right)^2 \left(\frac{h_s^2}{3} + H^2 + H h_s \right)}{A_d E \sigma_c^2 (1 - \nu) \left(2E e^{-bt} + \frac{\sigma_s^\mu}{B t^\omega} - \lambda \right)} \right) \sqrt{\frac{H_d^2}{H_d^2 + X^2}} \tag{5}$$

where x is the horizontal distance of the stress effect point from the panel edge.

Accordingly, the stress concentration factor k can be determined as follows (Rezaei et al. 2015b, c):

$$k = \frac{\sigma_v + (\sigma_v - \gamma H_d)}{\sigma_v} \sqrt{\frac{H_d^2}{H_d^2 + X^2}} \tag{6}$$

Physical modeling of longwall mining

Physical modeling allows researchers to observe development of ground movement, mining-induced stress, and fracture during excavation. Since it has a short test cycle and reliable result (Meguid et al. 2008; Jaiswal and Shrivastva 2004), this research method has been widely used in analyzing mining-related issues.

Similarity theory

In order to capture realistic behavior of strata during mining via physical modeling test, the model is required to be built in accordance with the principle of similarity theory. Moreover, the selection of raw materials and compounding ratios are the key matters in terms of mechanical properties of the modeling material.

The geometry ratio of the model to real stope should be firstly determined. Specifically, the dimension of the model, strength, and density of the modeling material need to match the following criterions (Yang et al. 2011; Meguid et al. 2008; Li 2016).

$$\frac{C_\sigma}{C_\rho \times C_L} = 1 \tag{7}$$

$$C_L = L_m / L_p, \quad C_\sigma = \sigma_m / \sigma_p, \quad C_\rho = \rho_m / \rho_p \tag{8}$$

where C_L is the geometry similarity constant, C_σ is the strength similarity constant, C_ρ is the density similarity constant, L is the geometric dimension, σ is the compressive strength, ρ is the density, the subscript P stands for prototype, and m stands for model.

Engineering background

In this research, Weijiagou Coal Mine was selected as prototype for physical modeling. This mine is located in the southwest China. The average slope angle and thickness of coal seam are 15° and 1.2 m which are adopted in the modeling design. The burial depth of coal seam is 530 m; the length of working face is 100 m. According to the synthetic stratum histogram, the overlying and underlying strata with similar lithology can be integrated into the following types: argillaceous sandstone, siltstone, mudstone, medium granular sandstone, sandy mudstone, and coal. The distribution and thickness of each stratum are shown in Fig. 2.

These similarity ratios of the scaled physical model are calculated and assigned according to the uniaxial compressive strength (UCS), physical characteristics, and

Table 1 The similarity ratios for the physical models

C_L	C_σ	C_ρ	q_m
1/60	1/90	1/1.5	8.36 kN

dimensions of the target prototype case. The final similarity ratios used in this experiment are noted in Table 1. q_m is the pressure of overlying strata beyond modeling scale applied on the top of the model.

Construction of physical modeling

In this research, sand-plaster-lime-water mixtures were utilized to simulate rock layers, and borax was proportionately added to delay the coagulation of plaster. By carrying out orthogonal experiment, the modeling material with different proportions of sand, lime, plaster, and water was tested. A part of the specimens and typical damage state are shown in Fig. 3. According to the similarity ratios, the compounding ratios for every lithology can be acquired (Table 2). Due to restrict of space, the details are not listed

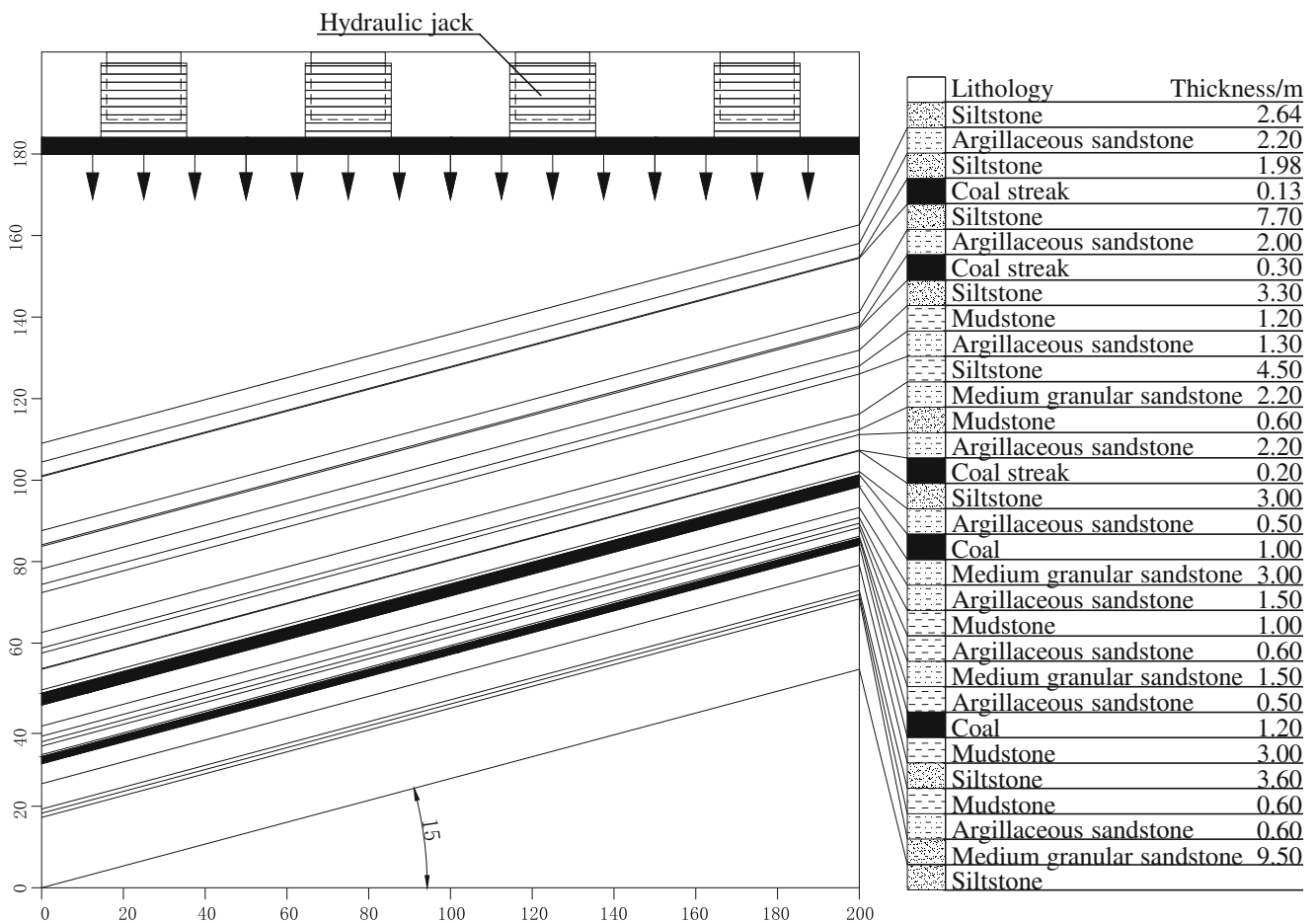


Fig. 2 The distribution of lithology and thickness of each strata

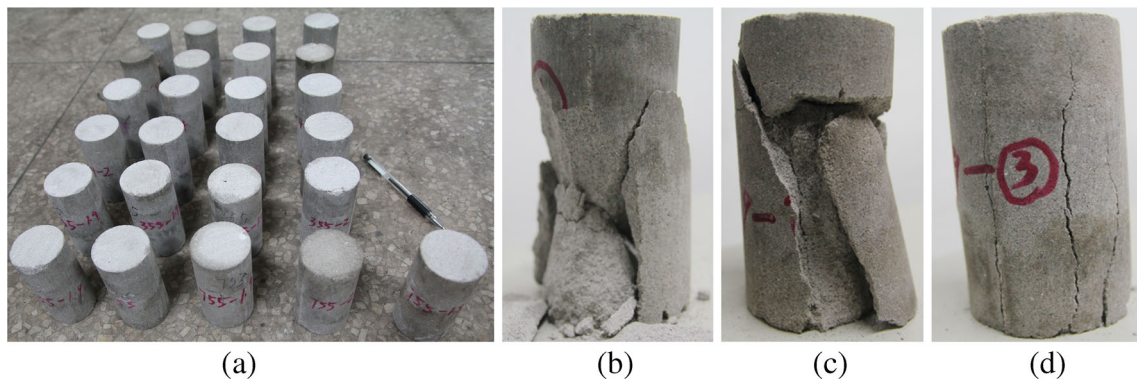


Fig. 3 The orthogonal experiment on compounding ratios: **a** Modeling material specimen. **b–d** The damage state of the specimen

here; readers can refer to the thesis of Li (2016) for more information.

In accord with the compounding ratios, the raw materials were evenly mixed and casted layer by layer in the self-developed rotatable physical similar test system (Fig. 4a). During the laying process, pressure cells (type SDTY-2) were buried in coal seam floor along dip direction and connected with strainmeter (type WS-3811, Fig. 4b) to collect strain data during excavation. The distance between each pressure cells was 0.07 m. After stacking the modeling material to the top of the frame, the model was fully air-dried. Before excavation, the displacement monitoring points were installed on the surface of the physical model to observe the deformation of strata during mining. The weight of overburden strata beyond the model scale was applied by hydraulic jacks. Digital photographs were used for measurement of the strata movement and crack propagation pattern by means of photogrammetry and digital image correlation (DIC) techniques. The layout of physical model is shown in Fig. 4a. Coal seam in the model was excavated via electric drill. Also, sufficient time was given between each step of excavation to allow the deformations to be fully developed.

Physical modeling results

Strata deformation

Since the deformation of strata significantly changed during coal seam excavation, displacement monitoring points can quantitatively display the deformation of strata. By taking pictures of the model in different mining stage, excavating the coordinates of monitoring points, calculating the increment of displacement, and importing the data into Sigmaplot, the deformation contour plot could be obtained (Fig. 5).

At the early stage, the excavation only caused deformation in adjacent strata around mining panel (Fig. 5a). As mining width increased, the deformation and movement of strata gradually developed from bottom to top of the overlying strata, while the increasing rate of the height of the distressed zone decreased (Fig. 5b, c). When the mining width exceeded 72 m, the excavation caused large-scale deformation of strata (Fig. 5d), and it developed to the top of the model.

Mining-induced crack propagation

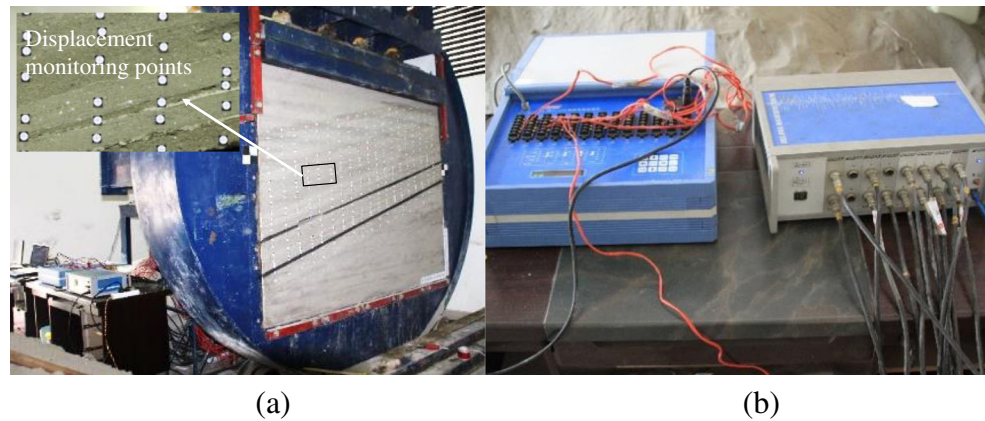
Coal seam mining results in crack propagation both in overlying and underlying strata. In order to acquire clear

Table 2 The compounding ratio and quality of the modeling materials for each rock layer

Lithology	Density g/cm ³	Compounding ratio	Compounding ratio			Water	Borax
			Sand	Lime	Plaster		
Argillaceous sandstone	1.900	1082	10	8	2	$m_{tot}/10^{-1*}$	$m_{tot}/10^{-3*}$
Siltstone	1.690	682	6	8	2	$m_{tot}/10^{-1*}$	$m_{tot}/10^{-3*}$
Mudstone	1.644	764	7	6	4	$m_{tot}/10^{-1*}$	$m_{tot}/10^{-3*}$
Medium granular sandstone	1.516	673	6	7	3	$m_{tot}/10^{-1*}$	$m_{tot}/10^{-3*}$
Sandy mudstone	1.580	1237	12	3	7	$m_{tot}/10^{-1*}$	$m_{tot}/10^{-3*}$
Coal	0.900	1428	14	2	8	$m_{tot}/10^{-1*}$	$m_{tot}/10^{-3*}$

* m_{tot} is the total quality

Fig. 4 The test system and instrument used in physical modeling experiment: **a** The self-developed rotatable physical similar test system. **b** The strainmeter used for stress monitoring



development of mining-induced crack, binarization method was used for manipulating photographs. Based on the modified photographs, the crack in different stages could be drawn as shown in Fig. 6. According to Fig. 6, it could be found that the connection of cracks resulted in separation and fracture of rock layers. At the early mining stage, only adjacent strata above stope caved (Fig. 6a). As mining width increased, the fracture propagated to the upper seam and generated destressed zone. Above this area, the intact rock strata only bended toward goaf (Fig. 6b). Judging from the spatial relationship between growth direction of crack and layout of strata, there were horizontal and perpendicular cracks in surrounding rock. The horizontal crack was generated by the separation of strata, and the perpendicular crack was produced by the fracture of layers. The height of caved zone firstly increased and become relatively unchanged when the crack propagated to the key stratum (Fig. 6c), similar to the variation of deformation. Generally, because of inclined occurrence of rock layers, the shape of the destressed zone was isosceles trapezoid when the stope reached balance. The next step of excavation re-activated the caved zone and generates new bedding separations and areas of crack closure and opening. Moreover, as the burial depth of the deeper end of working face was greater, the crack in this area appeared more congregated (Fig. 6d, section I and II). Finally, H_d was about 29.87 m.

Mining-induced stress concentration

Based on the monitoring data acquired from pressure cells that were buried in coal seam floor, the variation of stress concentration factor k could be calculated, as shown in Fig. 7.

Because coal seam mining caused stress relief, k appeared negative above goaf. Since the length of working face had a positive correlation with the volume of overlying strata of the destressed zone, the mining-induced stress became greater with mining width increased. The maximum of k in coal seam is about 1.94 in deep end of working face, and it was about 1.69 in shallow end when the mining width reached 72 m.

Comparative analysis

In order to carry out comparative analysis, the time-dependent energy model was used to calculate H_d and k . The utilized constant values in this calculation were referred to Rezaei et al. (2015a, c) and Zhang et al. (2011), as shown in Table 3.

The average bulking factor of overlying rock strata was set to 1.5. Generally, threshold value of stress was the yield point of stress-strain curve which was commonly assumed to be about 80% of the peak compressive stress (Falakian 2012). The pressure time of caved rock mass was set to 1.5 years (Rezaei et al. 2015a). Other geometrical and mechanical

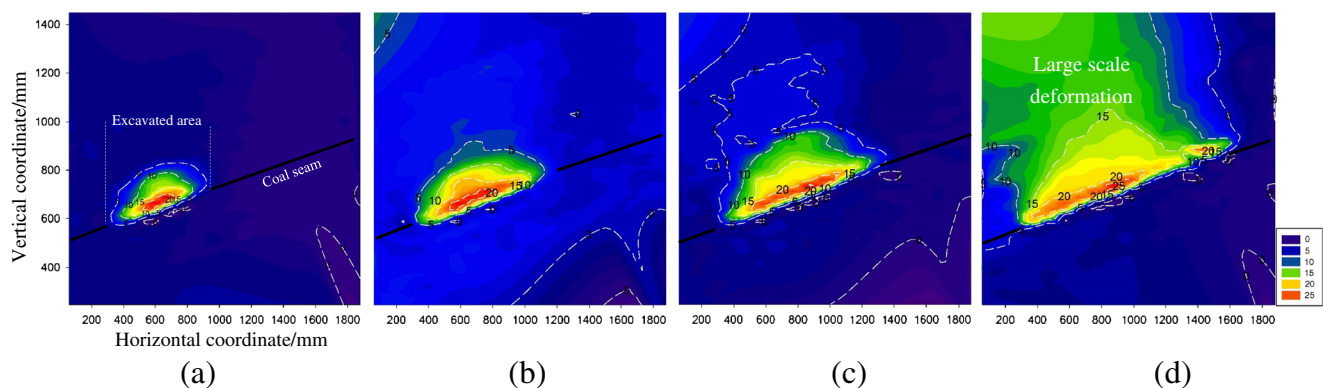


Fig. 5 Deformation contour plot of strata acquired by DIC technique at different mining width: **a** 36 m. **b** 60 m. **c** 72 m. **d** 90 m

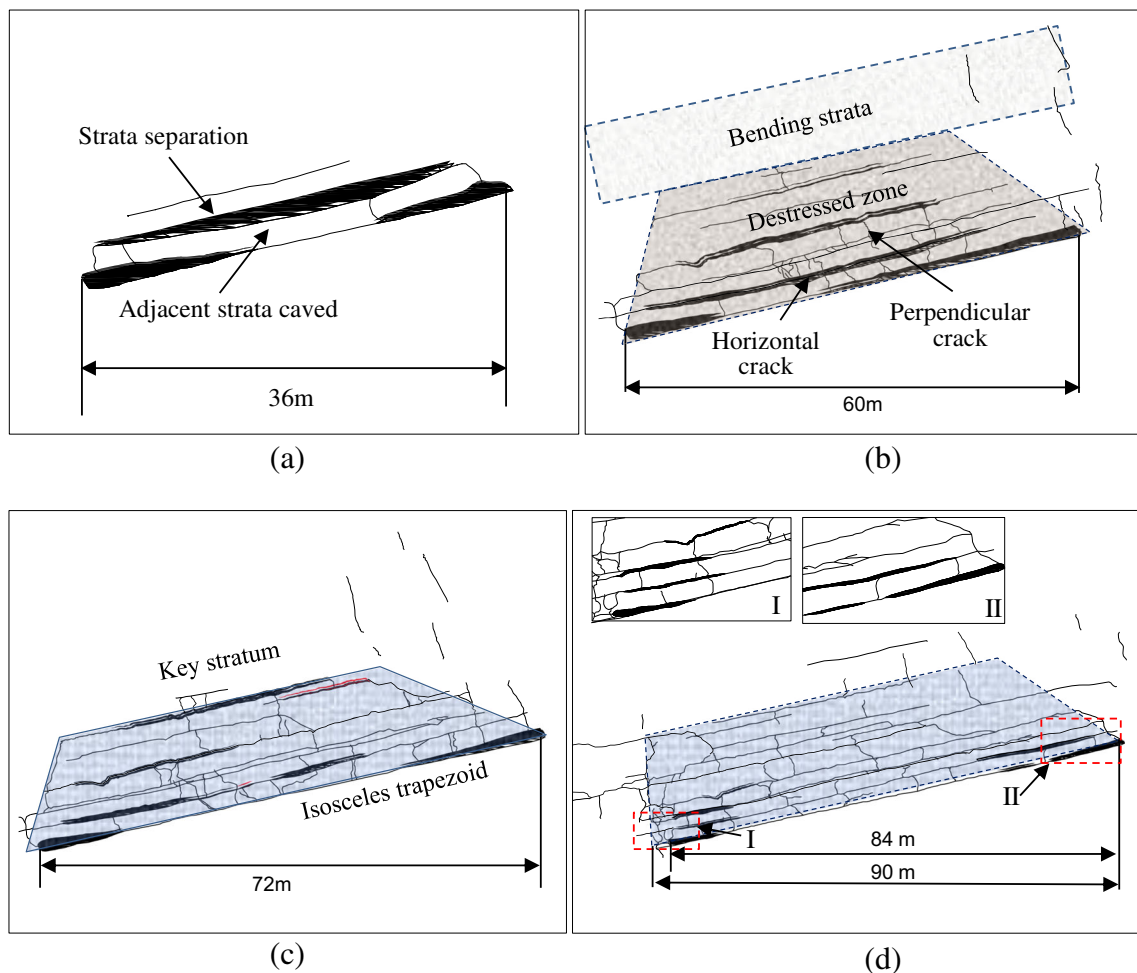


Fig. 6 The growth of mining-induced crack in surrounding rock

parameter values of coal seam and rock strata were listed in Table 4.

By taking the values of parameters into eqs. (4) and (6), the output of k was 2.13, and H_d was 23.53 m. When comparing with the modeling results, k obtained from the theoretical model was larger, but H_d was smaller. Generally, k had inverse relationship with the distance from the panel edge. Meanwhile, the panel edge was related to the length of working face. Because of the sidewall breakage of gate and pillars, which was widely existed in underground mining, actually, the length of working

face became greater. It increased the height of the destressed zone which generates a lower stress concentration. As shown in Fig. 6d, the deep end of working face damaged and caused an apparent decrease of stress concentrate (Fig. 7). Hence, the mining panel width should consider the plastic zone of the gate.

Hou and Ma (1989) proposed a method to calculate the width of the limit equilibrium zone of stress (i.e., the plastic zone x_0) as shown in the following equation:

$$x_0 = \frac{mA}{2\tan\phi_0} \ln \left(\frac{k\gamma H + \frac{C_0}{\tan\phi_0}}{\frac{C_0}{\tan\phi_0} + \frac{P_x}{A}} \right) \tag{9}$$

where C_0 and ϕ_0 were the fraction angle and cohesion between coal seam and rock layer (14° and 7.4 MPa), A was

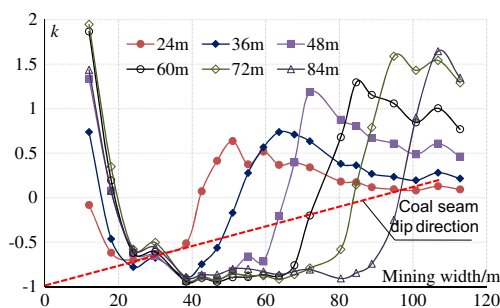


Fig. 7 The variation of stress concentration factor

Table 3 The value of experimental parameters used in calculation

B	μ	b	λ	ω	b_1
1.24	2	1	3	0.3	1.5

Table 4 Average values of geometrical and mechanical parameters

H/m	L_w/m	h_z/m	σ_c/MPa	γ/kNm^{-3}	ν	E/GPa	E_g/GPa	t/a
575	90	0.56	104.75	25	0.3	3.5	3	1.5

the ratio between horizontal and vertical stress (1.5), and p_x was supportive pressure (0.7 MPa).

Consequently, the equation of A_m could be modified as below:

$$A_m = (l_w + 2x_0)h_s \quad (10)$$

Based on the above modification, the values of H_d and k were 27.94 m and 1.82 which had a higher consistency with physical modeling. However, it should be noted that the presence of geological features, especially to the joints and faults, in different mining states led to variations in stress transfer and concentration. But, these geological features were not considered in the physical model and theoretical analysis as presented in this study. Actually, because of the initial damage existed in overlying strata, the height of the destressed zone may propagate higher.

Conclusions

In this research, in order to reveal the characteristics of deformation, damage, mining-induced stress, and crack in strata during long wall mining, the time-dependent energy model and physical modeling test were carried out based on the geological condition of Weijiagou Coal Mine. The physical modeling experiment was designed in accordance with the laws of similarity theory and conducted on the self-developed rotatable physical similar test system. Accordingly, the mechanical properties including strength and density of the modeling material were calculated. Orthogonal experiment method and mechanics tests were also performed to obtain the mechanical behavior of specimen with different compounding ratios. Accordingly, the best ratios for every lithology were determined.

Via the physical modeling experiment, strata movement, crack propagation, and mining-induced stress concentration during working face advancing were observed. The result showed that the deformation and crack developed to upper strata with mining width increase. But, the development stopped when the destressed zone grew to the bending strata. The excavation finally caused breakage of key strata, and it led to large-scale deformation of strata.

The structure of caved strata showed that the height of the destressed zone had a significant influence on stress distribution. When compared to the time-dependent energy model, the result obtained from physical modeling test indicated that the

height of the destressed zone was greater and the stress concentration factor was smaller. In order to reduce the deviation, the dimension of the plastic zone was introduced into mining panel width. Due to the modification, it drew a higher consistency with physical modeling.

Funding This research was supported by the National Natural Science Foundation of China (51474039, 51404046 and U1361205), program supported by the Fund of Chongqing Science and Technology Commission (cstc2015jcyjA90019), and the Science and Technology Research and Development Projects of Handan (1621211040-2, 1629209045-2).

Compliance with ethical standards

Conflict of interest The authors declare that they have no conflict of interest.

References

- Falakian A (2012) Experimental study of rock strength by using friction transfer method. *Indian J Sci Technol* 5(12):34–37
- Feng QJBS (2015) Analytical solution for stress and deformation of the mining floor based on integral transform. *Int J Min Sci Technol* 25(4):581–586. <https://doi.org/10.1016/j.ijmst.2015.05.010>
- Hou CJ, Ma NJ (1989) Stress in in-seam roadway sides and limit equilibrium zone. *J China Coal Soc* 4:21–29
- Jaiswal ASS, Shrivastva BK (2004) Numerical modeling study of asymmetry in the induced stresses over coal mine pillars with advancement of the goaf line. *Int J Rock Mechanics Mining Sci* 41(5):859–864. <https://doi.org/10.1016/j.ijmms.2004.01.007>
- Ju MH, Li XH, Yao QL, Liu SY, Liang S, Wang XL (2017) Effect of sand grain size on simulated mining-induced overburden failure in physical model tests. *Geology. on line, Engineering*
- Khanal M, Adhikary D (2012) Numerical analysis and geotechnical assessment of mine scale model. *Int J Min Sci Technol* 22(5):693–698. <https://doi.org/10.1016/j.ijmst.2012.08.017>
- Khanal M, Adhikary D, Rao B (2011) Evaluation of mine scale longwall top coal caving parameters using continuum analysis. *Min Sci Technol* 21(6):787–796
- Li GD (2016) The deformation mechanics of surrounding rock and supportive technology of secondary gob-side entry retaining [D]. Chongqing University, Chongqing
- Meguid MA, Saada O, Nunes MA, Mattar J (2008) Physical modeling of tunnels in soft ground: a review. *Tunn Undergr Space Technol* 23(2): 185–198. <https://doi.org/10.1016/j.tust.2007.02.003>
- Rezaei M, Hossaini MF, Majdi A (2015a) Development of a time-dependent energy model to calculate the mining induced stress over gates and pillars. *J Rock Mech Geotech Eng* 7(3):306–317. <https://doi.org/10.1016/j.jrmge.2015.01.001>
- Rezaei M, Hossaini MF, Majdi A (2015b) A time-independent energy model to determine the height of destressed zone above the mined panel in longwall coal mining. *Tunn Undergr Space Technol* 47:81–89. <https://doi.org/10.1016/j.tust.2015.01.001>
- Rezaei M, Hossaini MF, Majdi A (2015c) Determination of longwall mining induced stress using the strain energy method. *Rock Mech Rock Eng* 48(6):2421–2433. <https://doi.org/10.1007/s00603-014-0704-8>
- Salamon MDG (1984) Energy considerations in rock mechanics: fundamental results. *J South Afr Inst Min Metall* 84(8):233–246

- Singh GSP, Singh UK (2010) Prediction of caving behavior of strata and optimum rating of hydraulic powered support for longwall workings. *Int J Rock Mech Min Sci* 47(1):1–16. <https://doi.org/10.1016/j.ijrmms.2009.09.001>
- Toraño J, Díez RR, Cid JMR, MMC B, Casal Barciella MM (2002) FEM modeling of roadways driven in a fractured rock mass under a longwall influence. *Comput Geotech* 29(6):411–431. [https://doi.org/10.1016/S0266-352X\(02\)00006-X](https://doi.org/10.1016/S0266-352X(02)00006-X)
- Wang HW, Jiang YD, Xue S, Mao LT, Lin ZN, Deng DX, Zhang DQ (2016) Influence of fault slip on mining-induced pressure and optimization of roadway support design in fault-influenced zone. *J Rock Mech Geotech Eng* 8(5):660–671. <https://doi.org/10.1016/j.jrmge.2016.03.005>
- Yang W, Lin BQ, Qu YA, Li ZW, Zhai C, Jia L, Zhao W (2011) Stress evolution with time and space during mining of a coal seam. *Int J Rock Mech Min Sci* 48(7):1145–1152. <https://doi.org/10.1016/j.ijrmms.2011.07.006>
- Yavuz H (2004) An estimation method for cover pressure re-establishment distance and pressure distribution in the goaf of longwall mines. *Int J Rock Mechanics Min Sci* 41(2):193–205. [https://doi.org/10.1016/S1365-1609\(03\)00082-0](https://doi.org/10.1016/S1365-1609(03)00082-0)
- Zhang T, Ma M, Wang H, Xu H (2011) A nonlinear rheological model of backfill material for retaining roadways and the analysis of its stability. *Min Sci Technol* 21(4):543–546